#5932

AIR-SIDE PERFORMANCE OF ENHANCED BRAZED ALUMINUM HEAT EXCHANGERS

R.L. Webb, Ph.D., P.E.
Member ASHRAE

S.-H. Jung

ABSTRACT

This paper describes a brazed aluminum heat exchanger developed for air-cooled heat exchangers used in residential air conditioners and heat pumps. The brazed aluminum design provides higher performance per unit weight than currently used designs. Presently used indoor heat exchangers have plate fins on round tubes. The outdoor heat exchanger uses round tubes with either a plate fin or a spine fin geometry. The brazed aluminum heat exchanger is made of extruded aluminum tubes having a 1.0-in. (25-4 mm) major diameter and a 0.16-in. (4.06-mm) minor diameter. The tubes contain 0.031 in. (0.79 mm) thick membranes spaced at 0.194 in. (4.93 mm) to meet the R-22, 2,200 psi (15 MPa) design pressure. The air side uses the louvered fin geometry. Wind tunnel tests were made on two fin geometry variants, each having 12, 15, and 18 fins/in. (472, 591, and 709 fins/m). Compared to a 12 fpi (472 fins/m) plain plate fin with 3/8 in. (9.5 mm) diameter tubes, the brazed aluminum design gives a 90% higher heat transfer coefficient for only 25% high pressure drop. Compared to an 18 fpi (709 fins/m) spine fin design with 3/8 in. (9.5 mm) diameter tubes, the brazed aluminum design gives a 44% higher heat transfer coefficient and a 10% smaller pressure drop. Burst pressure tests showed that the tube failed at 1,900 psi (13 MPa). Increasing the membrane thickness to 0.036 in. (0.91 mm) will meet the required 2,200 psi (15 MPa) burst pressure.

INTRODUCTION

This paper describes a brazed aluminum heat exchanger developed for air-cooled heat exchangers used in residential air conditioners and heat pumps. The principal objective is to identify designs that provide higher performance per unit weight than currently used designs. Presently used indoor heat exchangers have plate fins on round tubes. The outdoor heat exchanger uses round tubes with either a plate fin or a spine fin geometry. Refrigerant evaporates on the tube side of the evaporator and condenses on the tube side of the condenser. Because the air-side thermal resistance is dominant, one seeks to use an "enhanced" surface geometry on the air side. Webb (1987) provides a description of typically used air-side enhancement geometries.

Our work progressed in two stages. First, we evaluated possible advanced air-side fin geometries applicable to round tubes. Second, we considered different heat exchanger design and construction concepts. As a result of these evaluations, we have identified a brazed aluminum heat exchanger using "flat" extruded aluminum tubes as the most promising design. Such a design is currently used in some automotive air-conditioning condensers. Webb and Gupte (1990) present a quantitative performance comparison of different fin geometries on round tubes relative to the brazed aluminum concept. That evaluation showed that the brazed aluminum heat exchanger offers significant weight reduction relative to currently used round-tube designs.

Figure 1 illustrates the core geometry of the brazed aluminum heat exchanger. It consists of a 0.16-in. (4.1-mm) minor diameter, flat aluminum tube having internal membranes. The air side has the louvered fin geometry. Louvered fins provide enhancement by the repeated growth and destruction of thin boundary layers on the short louver flow length. The louvers are typically 0.04 in. (1.0 mm) to 0.06 in. (1.5 mm). Figure 2 illustrates two competing concepts, both having interrupted, slit fins on 3/8-in. (9.5-mm) round tubes.

The Figure 1 flat-tube geometry offers significant advantages over the Figure 2 designs. They are:

1. The airflow is normal to all of the narrow strips on the Figure 1 geometry, which is not the case for the Figure 2a design. Further, the wake dissipation length decreases in the direction of the fin base in the Figure 2a geometry.
2. The fraction of the Figure 2b surface that is louvered is substantially smaller than in the Figure 1 geometry. If a greater area distribution of louvers were provided in the Figure 2b geometry, the fin efficiency would substantially decrease. This is because the slits would cut the heat conduction path from the round base tube.
3. A low velocity wake region occurs behind the tubes of the Figure 2a and 2b geometries. The heat transfer coefficient is substantially reduced in these regions, as documented by Webb (1990).
4. The low projected area of the Figure 1 flat tube will result in lower profile drag.

Ralph L. Webb, Ph.D., P.E., is a professor and **Sung-Han Jung** is a research assistant in the Department of Mechanical Engineering, Pennsylvania State University, University Park.

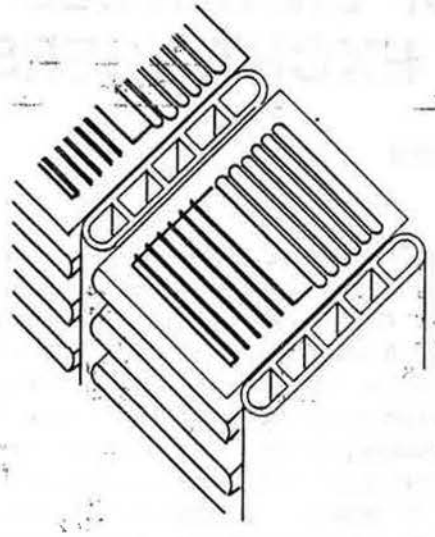

Figure 1 *Core geometry of the brazed aluminum heat exchanger.*

Some automotive air-conditioning condensers and evaporators currently use brazed aluminum heat exchangers having flat extruded aluminum tubes with internal membranes. The internal membranes are required to meet the 1,600-psi (11-MPa) burst pressure required for R-12 or R-134a used in automotive air conditioners. The presently considered application is for R-22 systems, which have higher burst pressure requirements. An R-22 system is designed for 2,200 psi (15 MPa). The failure mode of the flat tube/internal membrane geometry is by tension in the internal membranes. Hence, the internal membranes must be designed to withstand 2,200 psi (15 MPa) burst pressure.

BRAZED ALUMINUM HEAT EXCHANGERS TESTED

We have fabricated brazed aluminum heat exchangers and have obtained wind tunnel test data to define the air-side performance. In addition, tests have been conducted to establish the ability of the heat exchanger to drain condensate and to determine the burst pressure of the heat exchangers.

Figure 3 is a photograph of the brazed aluminum heat exchanger with standard fins. The fin material is clad with a braze alloy that melts at approximately 1100°F (593°C). The cladding thickness is approximately 15% of the total 0.006-in. (0.15-mm) fin stock thickness. A specially designed extruded aluminum tube was made for the heat exchangers. The extrusion, the fins, and the heat exchanger assembly and vacuum brazing were provided by a commercial supplier of similar heat exchangers for the automotive industry. Currently available fin geometries were used. However, the fin geometries were selected from a wide range of available choices to best meet the design guidelines described by Webb and Gupte (1990).

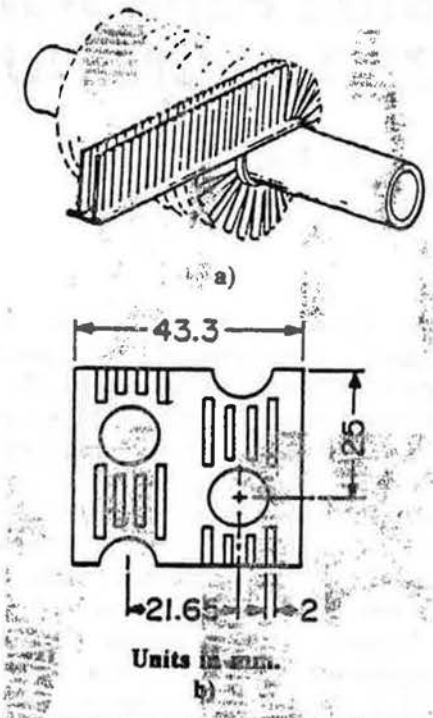

Figure 2 *Core geometry of round tube designs. (a) Spine-fin geometry; (b) slit fins.*

Each heat exchanger has approximately 22 in. (55.9 cm) by 15 in. (38.1 cm) frontal dimensions and contains two tube-side flow circuits. Two basic fin geometries were tested—the "standard" and the "splitter fin" types. Figures 4a and 4b show the standard and splitter fin surface geometries, respectively. The splitter fin geometry consists of two layers of 0.340 in. (8.6 mm) high fin material separated by a flat 0.0062 in. (0.16 mm) thick aluminum strip. Each geometry was made with fin densities of 12, 15, and 18 fins/in. (472, 591, and 709 fins/m), respectively. Table 1 describes the internal geometry of each design type.

Close inspection of the standard fins showed that the fin edges tended to be burred. Such burred fins have

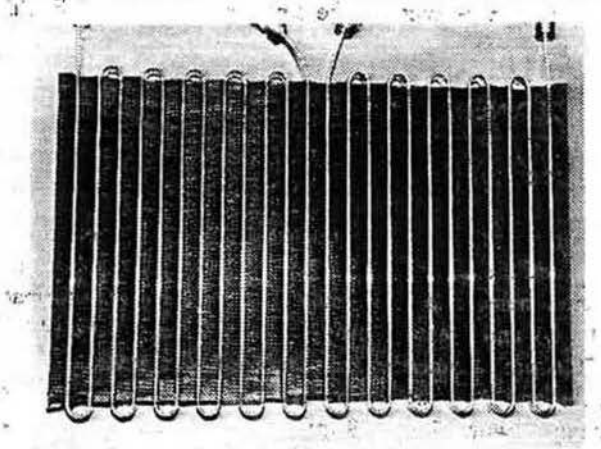

Figure 3 *Photograph of the 12 fins/in., 22.5 × 15.25 in. frontal area, standard fin geometry heat exchanger.*

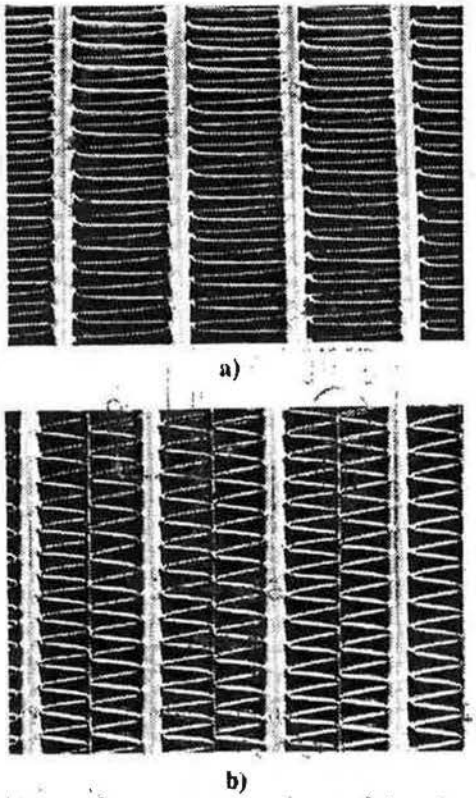

Figure 4 Photo of the fin arrays for 12 fins/in. (a) Standard fin geometry; (b) splitter fin geometry.

louvers with thinned, ragged trailing edges. The splitter fins showed no burrs.

Figure 5 shows the cross-sectional geometry of the tube. The tube cross section is 0.16 in. (4.06 mm) by 1.0 in. (25.4 mm) and has internal membranes at 0.194 in. (4.93 mm) pitch. The thickness of the tube wall and the membrane is 0.031 in. (0.79 mm).

Note that the louver pitch of the standard fin geometry is 0.055 in. (1.40 mm), relative to 0.04 in. (1.02 mm) for the splitter fin geometry. The smaller louver pitch should provide a higher heat transfer coefficient.

WIND TUNNEL TESTS

Test Procedure

Wind tunnel tests for the six cores have been completed, and the heat transfer rate and pressure drop data are presented here. The heat transfer coefficient (in the format $\eta h_o A_o/A_{fr}$) and pressure drop for the 12- and 18-fpi (472- and 709-fpm) geometries are compared with predicted heat transfer and pressure drop for plain and spine fin heat exchangers with 12 and 18 fpi (472 and 709 fpm), respectively.

The heat exchangers were tested in a draw-through wind tunnel using hot water on the tube side. The tunnel has a 12 × 18.75 in. (30.48 × 47.63 cm) rectangular cross section and a variable-speed fan that provides air velocities from 200 to 4,000 fpm (61 to 1,219 m/min). Room air is drawn in through an inlet section having a 12:1 contraction ratio and passes through the test heat exchanger. The leaving air temperature is measured by a grid of 24 thermocouples located 4 in. (10.2 cm) downstream from the heat exchanger. The air pressure drop is measured by a precision micromanometer. The air passes through a diffuser section and then to the variable-speed fan.

The water circulation loop supplies high-velocity hot water to the tube side. The water is heated by a 13.5-kW electric heater, whose power input is adjusted by a solid-state power controller. The water inlet/exit temperatures are measured by precision thermistors. The water flow rate was measured by a calibrated area flowmeter. The electric heat input to the water was adjusted to give an air tempera-

TABLE 1
Geometry of Cores Tested

Item	Standard	Splitter Fin
Heat Exchanger		
Core height (in.)	15.25	15.25
Core width (in.)	22.5	21.0
Tubes		
Major diameter (in.)	1.0	1.0
Minor diameter (in.)	0.16	0.16
Wall thickness (in.)	0.031	0.031
Tube pitch (in.)	0.91	0.85
Number of internal membranes	4	4
Internal membrane pitch (in.)	0.194	0.194
Internal membrane thickness (in.)	0.031	.031
Fins		
Fin height (in.)	0.745	Two layers of 0.34
Fin depth (in.)	1.03	1.03
Fin thickness (in.)	0.0062	0.0062
Louver pitch (in.)	0.055	0.04
Louver length/Fin height	0.8590	0.8220
Louver angle (deg)	30	30
Hydraulic diameter (in.)		
12 fpi	0.138	0.121
15 fpi	0.111	0.099
18 fpi	0.092	0.084
Contraction ratio (σ)		
12 fpi	0.762	0.743
15 fpi	0.747	0.728
18 fpi	0.732	0.714
Total heat transfer area/ Volume (β) (in.^{2}/in.^{3})		
12 fpi	22.23	24.72
15 fpi	27.15	29.43
18 fpi	32.08	34.19
Fin area/Total heat transfer area (A_f/A_o)		
12 fpi	0.895	0.899
15 fpi	0.914	0.915
18 fpi	0.927	0.927
Total heat transfer area/ Frontal area (A_o/A_{fr})		
12 fpi	22.90	25.46
15 fpi	27.97	30.32
18 fpi	33.04	35.21

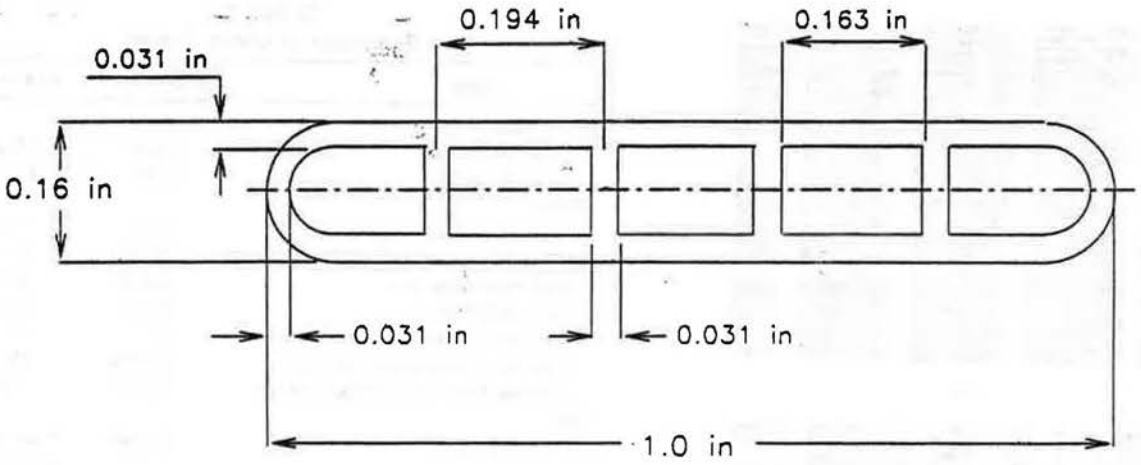

Figure 5 Cross-sectional geometry of the tube having 0.031 in. wall and membrane thickness.

ture rise of 10°F to 20°F (5.6°C to 11.1°C), with a minimum water temperature rise of 5°F (2.8°C). The heat input to the heat exchanger was calculated as the average received by the air and the heat loss from water. Heat balances were typically within ±2% to 4%.

The core width and height for the standard fin geometries were 22.5 in. (57.15 cm) by 15.25 in. (38.74 cm), while those for the splitter fin geometries were 21 in. (53.34 cm) by 15.25 in. (38.74 cm). Since the core width and height of the cores were longer than the wind tunnel test section (12 × 18.75 in. [30.48 × 47.63 cm]), wood frames were used to make the cores fit the wind tunnel cross section. The frames were sealed with tape on both sides to prevent air leakage.

Heat transfer coefficients were measured for air velocities between 235 and 3,200 fpm (72 and 975 m/min). The air pressure drop data were taken without heat transfer.

Reduced Data

The pressure drop data were reduced to obtain the Fanning friction factor. Entrance and exit losses to the core were subtracted. These losses were determined using Figure 5-2 from Kays and London (1984) for $Re_{Dh} = \infty$. The $Re_{Dh} = \infty$ condition is recommended by Kays and London for interrupted fins, which prevent a fully developed boundary layer.

The heat transfer rate (Q) is calculated as the average of the air- and water-side values. The UA-value was calculated using the effectiveness-NTU equation for unmixed-unmixed cross-flow. The air-side heat transfer coefficient was calculated by subtracting the water-side and the wall resistances from the total thermal resistance, assuming zero water-side fouling resistance. Thus,

$$\frac{A_{fr}}{\eta\, h_o A_o} = \frac{A_{fr}}{UA} - \frac{A_{fr}}{\eta_i h_i A_i} - \frac{A_{fr} t_w}{k_m A_w}. \qquad (1)$$

The Petukhov correlation for turbulent flow in tubes was used to calculate the tube-side heat transfer coefficient. This equation is

$$Nu_{Dh} = \frac{\left[\frac{f}{2}\right] Re_{Dh}\, Pr}{1.07 + 12.7\sqrt{\frac{f}{2}}\left(Pr^{2/3} - 1\right)} \qquad (2)$$

with the friction factor given by

$$f = \frac{1}{\left(1.58 \ln Re_{Dh} - 3.28\right)^2}. \qquad (3)$$

The Reynolds number used in Equation 2 is based on the hydraulic diameter of the internal passages in the extruded aluminum tube. Use of the hydraulic diameter for turbulent flow in noncircular tubes is well-accepted practice. The tube-side Reynolds number ranged from 13,300 to 23,350. The water-side thermal resistance varied from 3.0% at the lowest air velocity to 12.5% at the highest air velocity. The water-side membranes in the extruded tube act as fins. The calculated fin efficiency of the 0.049 in. (1.24 mm) high fins was calculated to be approximately 89%.

The air-side thermal resistance, $A_{fr}/\eta h_o A_o$, was "backed out" using Equation 1. The resulting $\eta h_o A_o/A_{fr}$ and pressure drop data were curve-fitted as a function of air frontal velocity. Figures 6a and 6b show $\eta h_o A_o/A_{fr}$ and Δp_{air} vs. u_{fr} (at 68°F [20°C]) for the standard and splitter fin geometries. The air-side fin efficiency ranged from 62% to 68%.

Figures 7 and 8 show j and f vs. Re_{Lp} for the standard and splitter fin cores, respectively. The air-side Reynolds number is based on the strip length (L_p) in the airflow direction. The choice of air-side hydraulic diameter or louver pitch for the characteristic dimension in the Reynolds number is arbitrary. We have chosen to use a Reynolds number based on strip length because it provides an approximate correlation of the heat transfer and friction data.

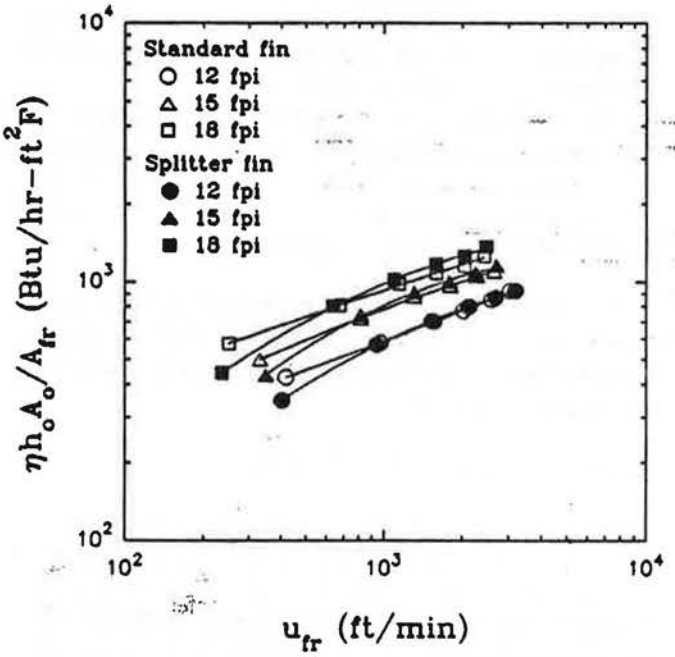

Figure 6a $\eta h_o A_o/A_{fr}$ *vs.* u_{fr} *(at 68°F) for the standard and splitter fin geometries.*

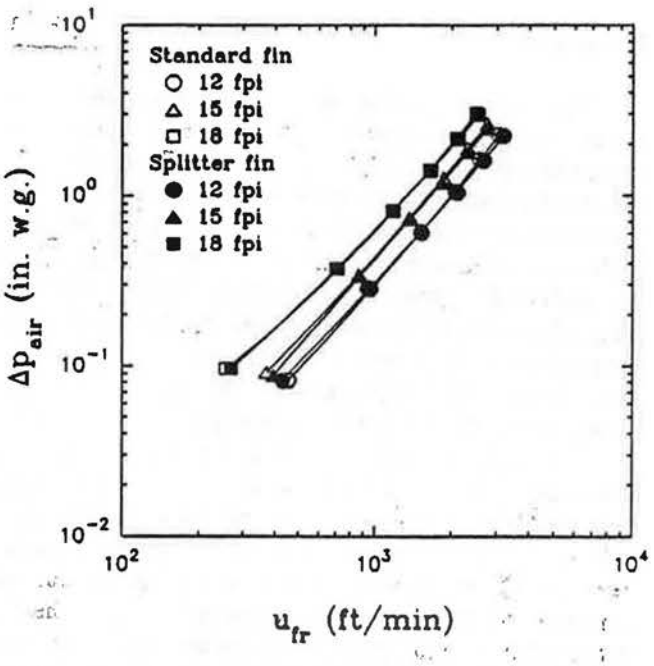

Figure 6b Δp_{air} *vs.* u_{fr} *(at 68°F) for the standard and splitter fin geometries.*

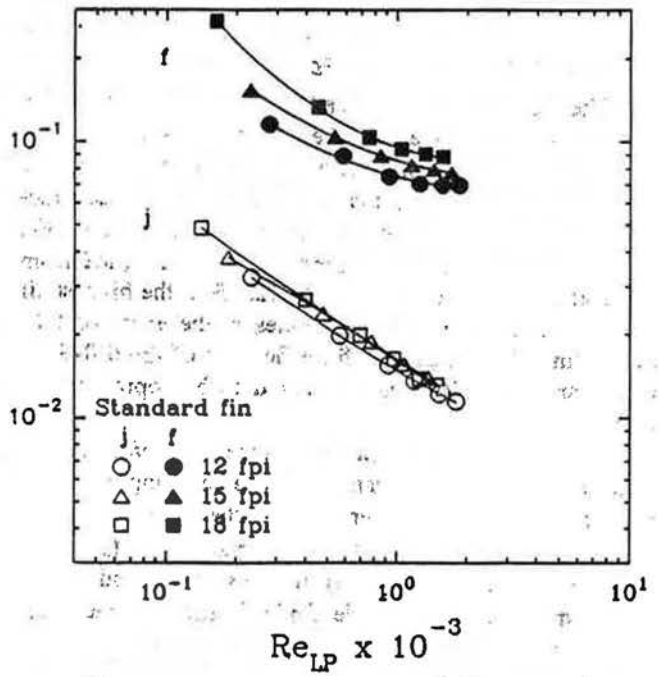

Louver pitch (in) = 0.055
Fin thickness (in) = 0.0062

	12 fpi	15fpi	18 fpi
Hydraulic diameter (in) =	0.138	0.111	0.092
Contraction ratio (σ) =	0.762	0.747	0.732
Fin area/total heat transfer area (A_f/A_o) =	0.895	0.914	0.927
Total heat transfer area/volume (β) (in^2/in^3) =	27.23	27.15	32.08
Total heat transfer area/frontal area (A_o/A_{fr}) =	22.90	27.97	33.04

Figure 7 j *and* f *vs.* Re_{LP} *plots for the standard fin cores.*

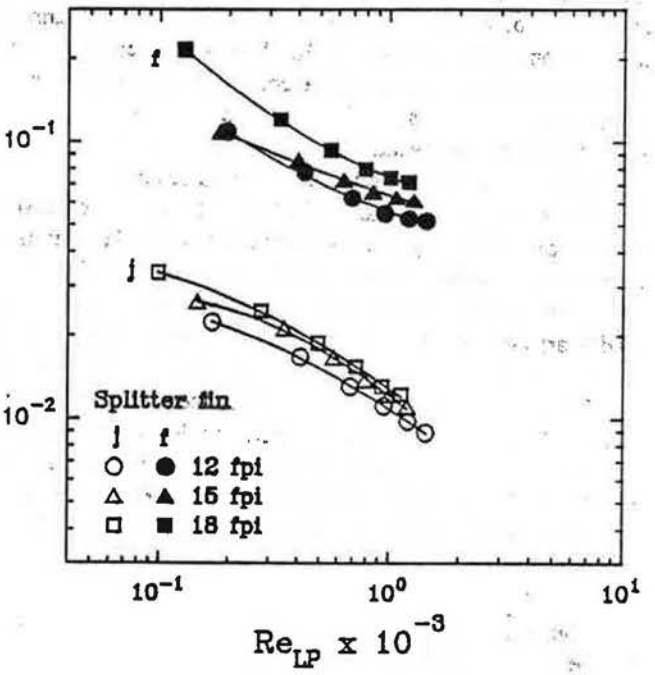

Louver pitch (in) = 0.04
Fin thickness (in) = 0.0062

	12 fpi	15fpi	18 fpi
Hydraulic diameter (in) =	0.121	0.099	0.084
Contraction ratio (σ) =	0.743	0.728	0.714
Fin area/total heat transfer area (A_f/A_o) =	0.899	0.915	0.927
Total heat transfer area/volume (β) (in^2/in^3) =	24.72	29.43	34.19
Total heat transfer area/frontal area (A_o/A_{fr}) =	25.46	30.32	35.21

Figure 8 j *and* f *vs.* Re_{LP} *plots for the splitter fin cores.*

Discussion

Figure 6b shows that the air-side pressure drop data for the standard fin geometry are almost equal or slightly higher than for the splitter fin geometry. Since the standard fins have a greater louver pitch than the splitter fins, one would expect lower pressure drop. It is probable that the higher than expected pressure drop of the standard fin is the result of the burred fin edges. Figure 6a shows that the $\eta h_o A_o/A_{fr}$ values of the standard fins are as high as those of the splitter fins, except at 18 fins/in. This is unexpected, since the standard fin geometry has approximately 10% less A_o/A_{fr} and a longer louver pitch than the splitter fin cores.

The $\eta h_o A_o/A_{fr}$ values for the splitter fin geometry fall below the standard fin values at the lower air velocities. This behavior was unexpected and may be due to the lower "flow efficiency" associated with the splitter fin geometry. The concept of flow efficiency applies to louver fin geometry and is discussed by Webb and Trauger (1991), who experimentally studied this phenomenon. At low Reynolds number and for large fin pitch-to-louver pitch ratio (F_p/L_p), they show that all of the flow does not pass over the louvers. Rather, some of the flow stream bypasses the louvers and flows as "duct flow" between the fin channels. For a given fin pitch, the splitter fin geometry has a larger F_p/L_p ratio than the standard fin core. As the air velocity is reduced, the friction factor of the louvers increases, which causes more of the flow to choose the duct flow path. This causes the heat transfer coefficient to decrease.

For a given fin pitch, the smaller louver pitch of the splitter fin geometry will result in smaller flow efficiency than for the standard fin, which has 38% greater louver pitch. However, the thermal performance of the splitter fin geometry decreases rapidly at the lowest air frontal velocity, where the "flow efficiency" for the standard fin geometry should also be low. This should also result in nonlinear (on log-log format) performance for the standard fin geometry. The data for the standard fin do not show such reduced performance. Presently, we do not understand why such reduced performance is not observed for the standard fin geometry at the lowest air velocity. It is possible that the burred fin edges of the standard fin geometry may be a factor.

COMPARISONS WITH CONVENTIONAL GEOMETRIES

The $\eta h_o A_o/A_{fr}$ and pressure drop for the present heat exchangers were compared with those for the Figure 2 spine and plain fin heat exchangers at the same air frontal velocities. The following comparisons were made:

1. The 12 fins/in. (472 fins/m) standard and splitter fin geometries were compared with a one-row, 12 fins/in. (472 fins/m) fin heat exchanger having plain fins and 3/8-in. (9.5-mm) outside diameter round tubes. A 12 fins/in. (472 fins/m) round tube geometry is typical of that used in indoor heat exchangers.
2. The 18 fins/in. (709 fins/m) standard and splitter fin geometries were compared with a one-row "spine fin" geometry having 18 fins/in. (709 fins/m) on 3/8-in. (9.5-mm) outside diameter round tubes. The spine fin is used in some outdoor heat exchangers.

The spine and plain fin geometries are summarized in Table 2, which provides fin geometry dimensions tested by Rabas and Eckels (1985), scaled values, and the values that are commercially used.

Correlation Used for the Spine Fin Geometry

Rabas and Eckels (1985) tested a one-row spine fin heat exchanger (Figure 2a) having D_{fin} = 1.374 in. (34.9 mm) on 0.50 in. (12.7 mm) O.D. tubes with P_t = 1.305 in. (33.1 mm). The heat exchanger had 20 fins/in. (787 fins/m), and the louver strip width (l_w) was 0.050 in. (1.27 mm) with 0.0080 in. (0.20 mm) fin thickness. The data on the 0.50 in. (12.7 mm) diameter tube spine fin would apply exactly to a 0.375 in. (9.5 mm) diameter spine fin if all the finned-tube dimensions are scaled by the ratio 0.375/0.500. The resulting scaled dimensions are D_{fin} = 1.03 in. (26.2 mm), P_t = 0.98 in. (24.9 mm), and l_w = 0.038 in. (0.97 mm) and 26.7 fins/in. (1051 fins/m). These dimensions are quite close to those of commercially used spine fin geometry. However, the commercial geometry uses approximately 20 fins/in. (787 fins/m).

We have used j and f vs. Re_D curve fits of the Rabas and Eckels (1985) spine fin to predict the performance of the 0.375-in. (9.5-mm) O.D. spine fin geometry of interest here. The curve fit equations are

$$j = 0.7728\ Re_D^{-0.491}, \quad (4)$$

$$f = 30.96\ Re_D^{-0.428} \text{ for } \sigma \le 0.4, \quad (5)$$

$$f = 27.88\ Re_D^{-0.454} \text{ for } \sigma \ge 0.4, \quad (6)$$

TABLE 2
Spine and Plain Fin Geometries

Item	Rabas (1985)	Spine Scaled	Commercial Spine Fin	Plain Fin
N_r	1	1	1	1
D_o (in.)	0.5	0.375	0.375	0.375
D_{fin} (in.)	1.374	1.031	1.23	N/A
P_t (in.)	1.305	0.979	1.16	0.893
P_l (in.)	N/A	N/A	N/A	0.774
t_f (in.)	0.008	0.006	0.006	0.006
l_w (in.)	0.05	0.0375	0.04	N/A
fpi	20	18	20	12

where

$$j = h_o \mathrm{Pr}^{2/3} / G_{max} c_p, \quad (7)$$

$$f = \Delta p_{air} \rho / 2 N_r G_{max}^2. \quad (8)$$

Correlation Used for the Plain Fin Geometry

The j and f vs. Re_{Dh} characteristics of the plain fin geometry are based on the test data of Rich (1973). Rich tested four-row plain plate fin-and-tube heat exchangers having 0.006 in. (0.15 mm) thick fins on 0.525 in. (13.3 mm) O.D. tubes. The tubes were equilaterally spaced on 1.25 in. (31.8 mm) centers. He tested eight different spacings, ranging from 2.92 to 20.6 fins/in. (115 to 811 fins/m). The j and f vs. Re_{Dh} curve for this geometry would apply exactly to 0.375 in. (9.5 mm) O.D. diameter tubes if all dimensions were reduced in the ratio of 0.375/0.525 = 0.714. This would give P_t = 0.893 in. (22.7 mm), P_l = 0.774 in. (19.7 mm), and t_f = 0.0043 in. (0.11 mm). Rich's 9.17 fins/in. (361 fins/m) scales to 12.84 fins/in. (506 fins/m). This is the closest fin pitch to the desired 12 fins/in. (472 fins/m). To predict the heat transfer coefficient for the 12 fins/in. (472 fins/m) core, we used the velocity in the minimum area of the 12 fins/in. (472 fins/m) core to calculate the Re_{Dh} and read the j factor for the 9.17 fins/in. (361 fins/m) core from Figure 10 in Rich's paper. Rich showed that the heat transfer coefficient is correlated by the velocity in the minimum area.

The desired 3/8 in. (9.5 mm) O.D., 12 fins/in. (472 fins/m) corresponds to 8.57 fins/in. (337 fins/m) for Rich's 0.525 in. (13.3 mm) coils. The f factors for the 9.17 fins/in. (361 fins/m) and 7.67 fins/in. (302 fins/m) were interpolated to predict the f factor for the 8.57 fins/in. (337 fins/m) core. Note that the air pressure drop for the plain fin geometry used in Table 4 is for a one-row core.

Comparison with the Spine and Plain Fin Geometries

The comparisons of the standard and splitter fin geometries with the spine and plain fin geometries (per row basis) were made at the same A_o/A_{fr}. The experimental j and f vs. u_{fr} for the standard and splitter fin cores were curve-fitted and used to calculate the $\eta h_o A_o/A_{fr}$ and pressure drop for the standard and splitter fin geometries with the same A_o/A_{fr} as that of plain or spine fin geometry. The core depth of the standard and splitter fin cores was calculated such that the A_o/A_{fr} value of the standard and splitter fin cores is identical to the A_o/A_{fr} value of the core to be compared.

Table 3 compares the $\eta h_o A_o/A_{fr}$ and pressure drop for the 18 fins/in. (709 fins/m) brazed aluminum heat exchangers with the 3/8 in. (9.5 mm) O.D., 18 fins/in. (709 fins/m) spine fin geometry. Table 4 compares the 12 fins/in. (472 fins/m) brazed aluminum heat exchangers with the 3/8 in. (9.5 mm) O.D., 12 fins/in. (472 fins/m) plain fin coils. The data in Tables 3 and 4 are graphically presented in Figures 9 and 10, respectively. Examination of Tables 3 and 4 shows that the standard fin geometry gives slightly higher heat transfer performance than the splitter fin at 350 fpm (107 m/min).

For the Table 3, 18 fins/in. (709 fins/m) comparison, the standard fin geometry provides 1.44 times higher $\eta h_o A_o/A_{fr}$ than the spine fin at 350 fpm (107 m/min) frontal velocity. The heat transfer increase, per unit pressure drop increase, is 1.60. At 350 fpm (107 m/min), the $\eta h_o A_o/A_{fr}$ increase of the splitter fin geometry is 4% less than for the standard fin geometry. This is because of the drop-off in performance of the splitter fin geometry at low air velocity. However, the splitter fin geometry

TABLE 3
Outdoor Heat Exchanger

Splitter (18 fpi) vs. Spine (18 fpi)
[Core depth (in.): Splitter (0.521), Spine (1.031)]

u_{fr} (fpm)	y (Btu/h·ft²·°F)	y/y_{sp}	Δp_{air} (in. w.g.)	$\Delta p_{air}/\Delta p_{air,sp}$
350	342	1.38	0.07	0.79
1000	612	1.55	0.33	0.74
2000	806	1.53	1.09	0.77

Standard (18 fpi) vs. Spine (18 fpi)
[Core depth (in.): Standard (0.557), Spine (1.031)]

u_{fr} (fpm)	y (Btu/h·ft²·°F)	y/y_{sp}	Δp_{air} (in. w.g.)	$\Delta p_{air}/\Delta p_{air,sp}$
350	359	1.44	0.08	0.90
1000	515	1.30	0.33	0.75
2000	627	1.19	1.10	0.85

where
y = $\eta h_o A_o/A_{fr}$
sp = spine fin

TABLE 4
Indoor Heat Exchanger

Splitter (12 fpi) vs. Plain (12 fpi)
[Core depth (in.): Splitter (0.672), Plain (0.774)]

u_{fr} (fpm)	y (Btu/h·ft²·°F)	y/y_{pl}	Δp_{air} (in. w.g.)	$\Delta p_{air}/\Delta p_{air,pl}$
350	232	1.68	0.04	1.22
600	342	1.81	0.09	1.22
1000	455	1.72	0.21	1.13
2000	626	1.59	0.64	1.02

Standard (12 fpi) vs. Plain (12 fpi)
[Core depth (in.): Standard (0.752), Plain (0.774)]

u_{fr} (fpm)	y (Btu/h·ft²·°F)	y/y_{pl}	Δp_{air} (in. w.g.)	$\Delta p_{air}/\Delta p_{air,pl}$
350	309	2.23	0.04	1.18
600	360	1.90	0.09	1.25
1000	434	1.63	0.22	1.19
2000	563	1.43	0.72	1.15

where
y = $\eta h_o A_o/A_{fr}$
pl = plain fin

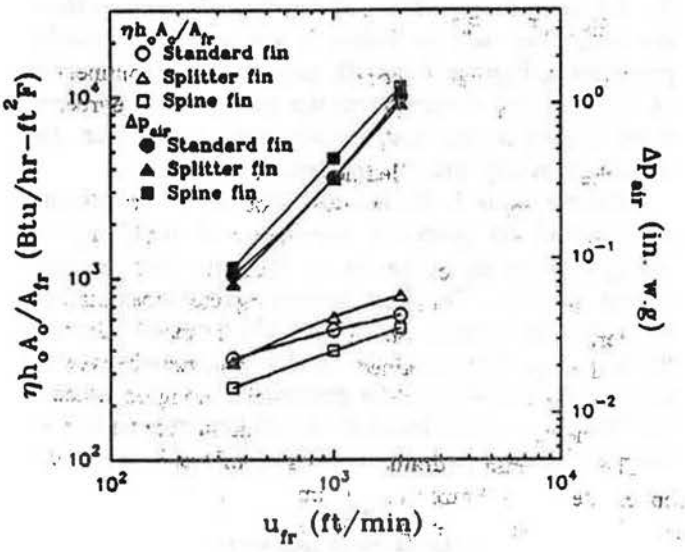

	Standard	Splitter	Spine
Core depth (in) =	0.557	0.521	1.031
Total heat transfer area/frontal area (A_o/A_{fr}) =	17.93	17.93	17.93

Figure 9 $\eta h_o A_o/A_{fr}$ *and* Δp_{air} *vs.* u_{fr} *(at 68°F) for the 18-fpi brazed aluminum and the spine fin heat exchangers.*

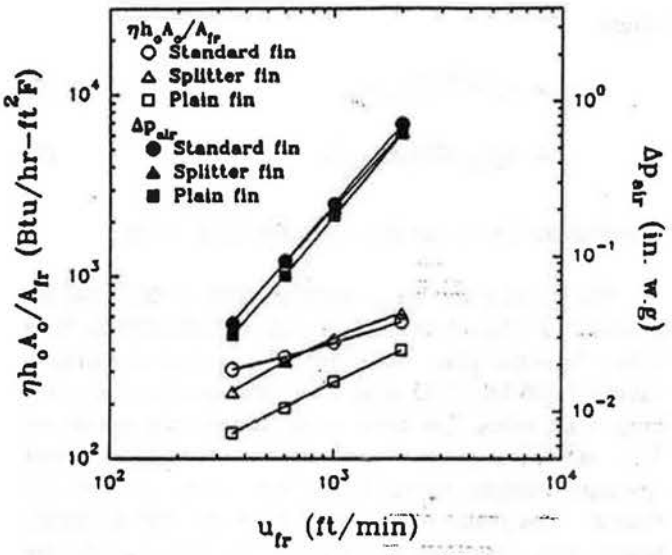

	Standard	Splitter	Plain
Core depth (in) =	0.752	0.672	0.774
Total heat transfer area/frontal area (A_o/A_{fr}) =	16.68	16.68	16.68

Figure 10 $\eta h_o A_o/A_{fr}$ *and* Δp_{air} *vs.* u_{fr} *(at 68°F) for the 12-fpi brazed aluminum and the plain fin heat exchangers.*

actually gives higher $\eta h_o A_o/A_{fr}$ per unit pressure drop than is obtained by the standard fin geometry. At 350 fpm (107 m/min), the air-side heat transfer increase is 75% more than the pressure drop increase (1.38/0.79). To obtain equal $\eta h_o A_o/A_{fr}$, the brazed standard aluminum core depth would be only 35% that of the 3/8 in. (9.5 mm) O.D. spine fin coil [0.521/(1.03 × 1.44)], and the pressure drop would be 63% that of the spine fin (0.90/1.44). At 1,000 fpm (305 m/min), the performance of the splitter fin is superior to the standard fin in terms of both heat transfer and pressure drop.

Table 4 compares the brazed aluminum geometries against the 3/8 in. (9.5 mm) O.D. plain plate fin geometry. Consider the performance comparison for 600 fpm (183 m/min), which is typical of the velocity for the indoor coil. The $\eta h_o A_o/A_{fr}$ of the standard fin geometry is 1.90 times that of the plain fin geometry, and the pressure drop is 1.25 times that of the plain fin coil. The heat transfer increase, per unit pressure drop increase, is 1.52 (1.90/1.25). To obtain equal $\eta h_o A_o/A_{fr}$, the brazed standard aluminum core depth would be only 51% that of the 3/8 in. (9.5 mm) O.D. plain plate fin coil [0.752/(0.774 × 1.90)], and the pressure drop would be 66% that of the plain fin (1.25/1.90).

Hence, we conclude that the brazed aluminum design offers significant performance advantage over the designs currently used in indoor and outdoor heat exchangers. The brazed aluminum heat exchanger may be used to obtain either material and size reduction or frontal area reduction.

BURST PRESSURE TESTS

The tubes were extruded from an alloy whose tensile strength is 13,900 psi (96 MPa) and yield stress is 4,400 psi (30 MPa). Mechanical strength analysis shows that the weakest point of the heat exchanger is the internal tube membrane, which is under tension. The membrane thickness was designed to withstand 2,200 psi (15 MPa) internal pressure. The original design analysis was based on 16,000 psi (110 MPa) tensile stress, which is higher than the 13,900 psi (96 MPa) strength of the alloy from which the tubes were made. The burst pressure predicted for the alloy used is 3,176 psi (22 MPa) for tensile failure of the membranes. It is calculated for tension on six membranes (four internal and two at the ends) by the equation

$$p = \frac{13{,}900 \times 6 \times 0.031}{1 - 6 \times 0.031} = 3{,}176 \text{ psi.} \qquad (9)$$

Analysis of the heat exchanger design showed that the highest stress on the membranes exists at the transition fitting, which is shown in Figure 11. The pressure load in the fitting is transmitted to the membranes, which causes increased stress on the membranes in the vicinity of the transition fitting. Hence, the heat exchanger is expected to fail in the membranes adjacent to the transition fitting. The burst pressure should be less than that predicted by Equation 9. Thus, the design of the transition fitting should affect the burst pressure.

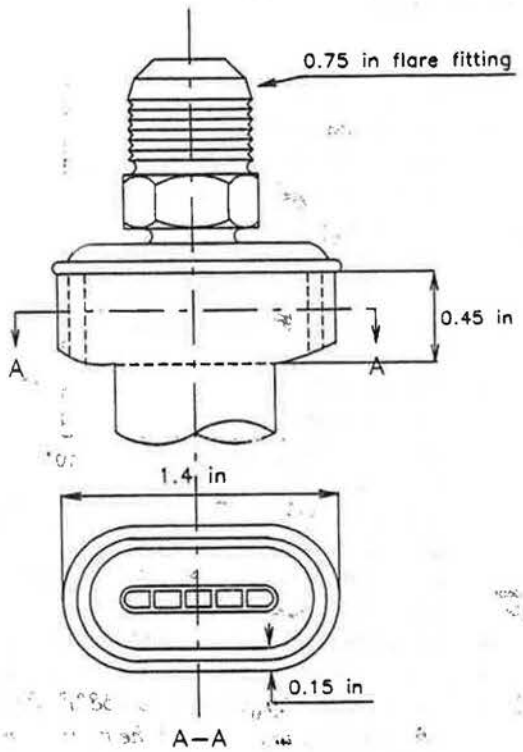

Figure 11 Cross-sectional geometry of the transition fitting.

Initial burst pressure tests were performed on three of the brazed aluminum heat exchangers. In all tests, the tube ruptured in the joint of the transition fitting. The observed burst pressures were one at 1,800 (12 MPa) and two at 2,000 psi (14 MPa). The 2,000-psi (14-MPa) burst pressure is 63% of the predicted value. Detailed examination of the failure showed that failure occurred at the inlet transition fitting. The fitting expanded to approximately 0.4 in. (10.2 mm) over a 0.7 in. (17.8 mm) tube length. A crack occurred in the braze in the minor tube diameter. As anticipated, the burst pressure was controlled by the design of the transition fitting. It is possible to identify a higher strength design for the transition fitting.

We next wished to determine the burst pressure of the tube separate from factors influenced by the transition fitting design. This was accomplished by clamping backing plates to the tube adjacent to the transition fitting. This removed the high stress on the internal membranes caused by pressure in the fitting. Two burst pressure tests were conducted. In these two tests, the tube failed at 1,900 psi (13 MPa) and 1,950 psi (13.4 MPa), respectively. The failure occurred at the U-bend region of the aluminum tube. These lower than predicted burst pressures are probably due to the residual stress in the U-bend region.

If the membrane thickness is increased from 0.031 in. (0.79 mm) to 0.036 in. (0.91 mm), the required 2,200 psi (15 MPa) burst pressure should be met.

CONDENSATE DRAINAGE TESTS

The 18-fpi splitter fin core was installed in a commercial vertical air handler. The core was tilted 63 degrees from the horizontal plane. The angle used is the same as that of the originally installed heat exchanger.

The air frontal velocity was about 350 fpm (107 m/min) during the tests. Condensation occurred on both the tube and the fins. The condensation on the tube was mainly filmwise and periodically drained along the tube minor diameter. The condensation on the fins was mainly dropwise and periodically drained through the gaps between louvers by gravity, when the small droplets conglomerated and became heavy enough to overcome the surface tension.

The condensate drainage tests confirmed that the condensate on the brazed aluminum geometry would drain as well as in existing evaporator geometries.

FUTURE WORK

The present program has shown that the air-side performance of the brazed aluminum heat exchanger provides performance and weight advantages over the commercially used round tube designs (Figure 2). It is possible that the air-side performance can be further improved. The potential cost advantage is yet to be determined. The heat exchanger cost is composed of the material cost and the assembly/brazing cost. Based on private discussions with automotive industry engineers, the brazing cost may be approximately 35% of the total cost.

Additional work is required to quantify the refrigerant-side heat transfer and pressure drop performance. It is possible that the tube may be extruded with a "micro-fin" internal surface geometry. This would enhance the tube-side performance. The incremental cost of providing the micro-fin internal geometry is very small. The Figure 2 round tubes typically use the micro-fin surface geometry. The micro-fin geometry consists of small fins of triangular cross section at a helix angle of 0° to 18° (measured from the tube center line). A 3/8-in. (9.5-mm) tube typically has 60 fins 0.008 in. (0.20 mm) high. This same fin geometry can be provided in the extruded aluminum tube with a 0.0° helix angle. The microfin tube geometry and its performance are described by Shinohara and Tobe (1985) and Schlager et al. (1989). Such extruded aluminum tubes with micro-fins are used in some automotive refrigerant condensers.

It is possible that the cost of heat exchanger material can be reduced by providing the brazing alloy cladding on the tube rather than on the fin material. The clad fin material cost is approximately $0.40/lb ($0.88/kg) more than unclad fin material, based on $1.25/lb ($2.76/kg) or aluminum fin strip. Presently, all aluminum finned-tube heat exchangers made with round aluminum tubes use clad tubes rather than clad fins. The tubes are made from clad strip, which is seam welded. Process development is under way in the aluminum industry that will allow cladding on extrusions of the tube type used here.

Higher strength alloys are available for the extrusion. The strength of the alloy used to make the extrusion is approximately equal to that of 3003 alloy. The use of heat-treatable alloys is also a possibility.

CONCLUSIONS

1. For 18 fins/in. (709 fins/m) and the same A_o/A_{fr} as the 3/8 in. (9.5 mm) O.D. spine fin, comparison at 350 fpm (107 m/min) shows:
   a. The $\eta h_o A_o/A_{fr}$ for the splitter fin geometry is 1.38 times that of the spine fin geometry. The heat transfer increase is 75% more than the pressure drop increase.
   b. The $\eta h_o A_o/A_{fr}$ for the standard fin geometry is 1.44 times that of the spine fin geometry. The heat transfer increase is 60% more than the pressure drop increase.
2. For 12 fins/in. (472 fins/m) and the same A_o/A_{fr} as the 3/8 in. (9.5 mm) O.D. plain plate fin, comparison at 600 fpm (183 m/min) shows:
   a. The $\eta h_o A_o/A_{fr}$ for the splitter fin geometry is 1.81 times that of the plain fin geometry. The heat transfer increase is 48% more than the pressure drop increase.
   b. The $\eta h_o A_o/A_{fr}$ for the standard fin geometry is 1.90 times that of the plain fin geometry. The heat transfer increase is 52% more than the pressure drop increase.
3. The standard and splitter fin heat exchangers should provide significant weight or frontal area reductions compared to the presently used round-tube heat exchanger designs. The brazed aluminum heat exchangers are applicable to both outdoor and indoor heat exchangers.
4. The observed burst pressures were between 1,800 (12 MPa) and 2,000 psi (14 MPa). The required 2,200-psi (15-MPa) burst pressure should be satisfied by increasing the membrane thickness from 0.031 in. (0.79 mm) to 0.036 in. (0.91 mm).
5. The proposed geometries drain condensate successfully.
6. Choice of the standard or splitter fin should be based on performance and cost considerations. Although the column strength of the splitter fin is greater than that of the standard fin, this increased strength is not used because the internal tube pressure is restrained by the tube's internal membranes.

ACKNOWLEDGMENT

Support for this research was provided by the Electric Power Research Institute (EPRI) under grant no. RP2792-16. The support of Dr. P.A. Joyner, EPRI Program Manager, is gratefully acknowledged. The heat exchangers were fabricated by Thermal Components, Inc., Montgomery, AL.

NOMENCLATURE

A_f	=	fin area (in.^{2})
A_{fr}	=	airflow frontal area (in.^{2})
A_i	=	water-side surface area (in.^{2})
A_o	=	air-side surface area (in.^{2})
A_w	=	conduction area in tube wall (in.^{2})
c_p	=	specific heat (Btu/lb·°F)
D_{fin}	=	diameter over spine fins (in.)
D_o	=	outside diameter of tube (in.)
f	=	Fanning friction factor (dimensionless)
F_p	=	fin pitch (in.)
fpi	=	fins per inch
fpm	=	fins per meter
G_{max}	=	mass velocity in minimum flow area (lbm/ft^2·h)
HB	=	heat balance $(Q_{wat} - Q_{air})/Q_{wat}$, dimensionless
h_i	=	water-side heat transfer coefficient (Btu/h·ft^2·°F)
h_o	=	air-side heat transfer coefficient (Btu/h·ft^2·°F)
j	=	j factor defined by Equation 7 (dimensionless)
k_m	=	thermal conductivity of tube (Btu/h·ft·°F)
L_p	=	louver pitch (in.)
l_w	=	width of louver or spine (in.)
Nu_{Dh}	=	Nusselt number based on hydraulic diameter (dimensionless)
N_r	=	number of rows in heat exchanger
p	=	pressure (lb$_f$/in.^{2})
Pr	=	Prandtl number (dimensionless)
pl	=	subscript to identify plain fin
P_l	=	longitudinal tube pitch (in.)
P_t	=	transverse tube pitch (in.)
Q	=	heat transfer rate (Btu/h)
Q_{air}	=	heat transferred to air (Btu/h)
Q_{wat}	=	heat rejected from water (Btu/h)
Re_D	=	Reynolds number based on fin collar diameter (dimensionless)
Re_{Dh}	=	Reynolds number based on hydraulic diameter (dimensionless)
Re_{LP}	=	Reynolds number based on louver pitch (dimensionless)
sp	=	subscript used to identify spine fin geometry
t_f	=	fin thickness (in.)
t_w	=	tube wall thickness (in.)
u_{fr}	=	air frontal velocity (fpm)
U	=	overall heat transfer coefficient (Btu/h·ft^2·°F)
y	=	$\eta h_o A_o/A_{fr}$ (Btu/h·ft^2·°F)

Greek Symbols

η	=	surface efficiency for air side (dimensionless)
η_i	=	surface efficiency for water side (dimensionless)
Δp_{air}	=	air pressure drop (in. w.g.)
σ	=	contraction ratio (dimensionless)

β = total heat transfer area/volume ($in.^2/in.^3$)
ρ = density (lb_m/ft^3)

REFERENCES

Kays, W.M., and A.L. London. 1984. *Compact heat exchangers*, 3d ed. New York: McGraw-Hill.

Rabas, T.J., and P.W. Eckels. 1985. Heat transfer and pressure drop performance of segmented surface tube bundles. ASME Paper 75-HT-45.

Rich, D.G. 1973. The effect of fin spacing on the heat transfer and friction performance of multi-row, smooth plate fin-and-tube heat exchangers. *ASHRAE Transactions* 79(2).

Schlager, L.M., M.B. Pate, and A.E. Bergles. 1989. Performance of micro-fin tubes with refrigerant-22 and oil mixtures. *ASHRAE Journal* 31(11): 17-28.

Shinohara, Y., and M. Tobe. 1985. Development of an improved thermo-fin tube. *Hitachi Cable Review* No. 4, pp. 47-50.

Webb, R.L. 1983. Heat transfer and friction characteristics for finned tubes having plain fins. In *Low Reynolds Number Flow Heat Exchangers*, eds. S. Kakac, R.K. Shah, and A.E. Bergles, pp. 431-450. Washington, DC: Hemisphere Publishing Co.

Webb, R.L. 1987. Enhancement of single-phase heat transfer, chapter 17 in *Handbook of Single-Phase Heat Transfer*, S. Kakac, R.K. Shah, and W. Aung, eds. New York: John Wiley & Sons.

Webb, R.L. 1990. Air-side heat transfer correlations for flat and wavy plate fin-and-tube geometries. *ASHRAE Transactions* 96(2): 445-449.

Webb, R.L., and N. Gupte. 1990. Design of light weight heat exchangers for air-to-two phase service. *Compact Heat Exchangers: A Festschrift for A.L. London*, R.K. Shah, A. Kraus, and D.E. Metzger, eds., pp. 311-334. Washington, DC: Hemisphere Publishing Corp.

Webb, R.L., and P. Trauger. 1991. Flow structure in the louvered fin heat exchanger geometry. *Experimental Thermal and Fluid Science* 4: 205-217.